Report

Current Biology

A pH-powered mechanochemical engine regulates the buoyancy of *Chaoborus* midge larvae

Graphical abstract

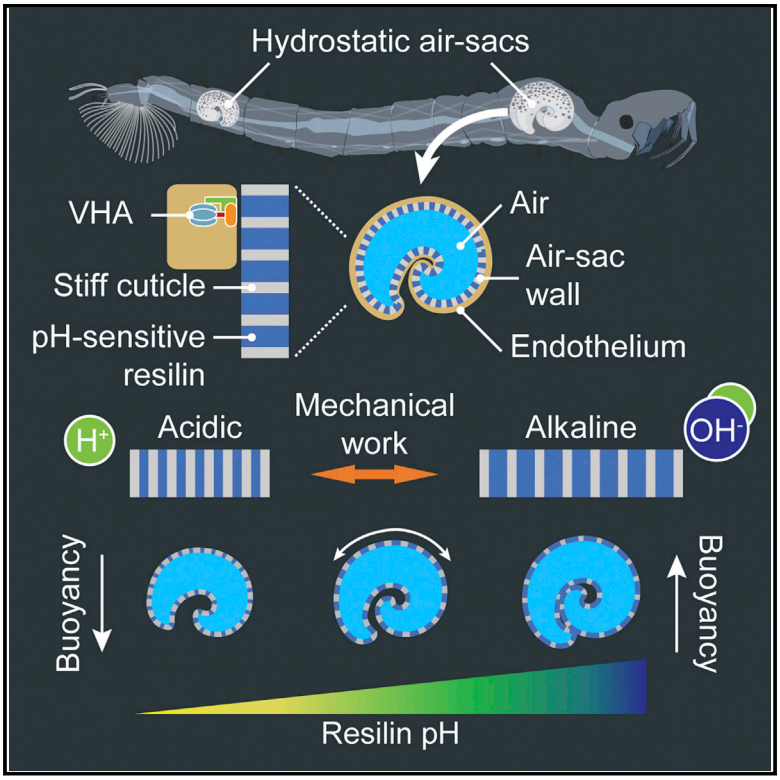

Authors

Evan K.G. McKenzie, Garfield T. Kwan, Martin Tresguerres, Philip G.D. Matthews

Correspondence

emckenzie@zoology.ubc.ca

In brief

Aquatic larvae of the *Chaoborus* midge are the only truly planktonic insects, regulating their buoyancy using air-filled sacs. McKenzie et al. find that the air-sac's volume is altered by bands of resilin in the sac wall, which contract in response to acidification driven by endothelial VHA and expand in response to alkalinization triggered by cyclic AMP (cAMP).

Highlights

- Aquatic *Chaoborus* midge larvae regulate their buoyancy using tracheal air-sacs
- pH-induced swelling of resilin bands in the air-sac wall alters the sac's volume
- Resilin pH is regulated by VHA H^+ pumps antagonized by the cAMP signaling pathway
- The air-sac behaves as a pH muscle as the resilin bands swell in one dimension only

McKenzie et al., 2022, Current Biology *32*, 1–7
February 28, 2022
https://doi.org/10.1016/j.cub.2022.01.018

CellPress

Please cite this article in press as: McKenzie et al., A pH-powered mechanochemical engine regulates the buoyancy of *Chaoborus* midge larvae, Current Biology (2022), https://doi.org/10.1016/j.cub.2022.01.018

Current Biology

CellPress

Report

A pH-powered mechanochemical engine regulates the buoyancy of *Chaoborus* midge larvae

Evan K.G. McKenzie,[1,3,4,*] Garfield T. Kwan,[2] Martin Tresguerres,[2] and Philip G.D. Matthews[1]
[1]Department of Zoology, The University of British Columbia, Vancouver, Canada
[2]Scripps Institution of Oceanography, University of California, San Diego, San Diego, CA, USA
[3]Twitter: @EvanMcK6
[4]Lead contact
*Correspondence: emckenzie@zoology.ubc.ca
https://doi.org/10.1016/j.cub.2022.01.018

SUMMARY

The freshwater aquatic larvae of the *Chaoborus* midge are the world's only truly planktonic insects, regulating their buoyancy using two pairs of internal air-filled sacs, one in the thorax and the other in the seventh abdominal segment. In 1911, August Krogh demonstrated the larvae's ability to control their buoyancy by exposing them to an increase in hydrostatic pressure.[1] However, how these insects control the volume of their air-sacs has remained a mystery. Gas is not secreted into the air-sacs, as the luminal gas composition is always the same as that dissolved in the surrounding water.[1,2] Instead, the air-sac wall was thought to play some role.[3–6] Here we reveal that bands of resilin in the air-sac's wall are responsible for the changes in volume. These bands expand and contract in response to changes in pH generated by an endothelium that envelops the air-sac. Vacuolar type H^+ V-ATPase (VHA) in the endothelium acidifies and shrinks the air-sac, while alkalinization and expansion are regulated by the cyclic adenosine monophosphate signal transduction pathway. Thus, *Chaoborus* air-sacs function as mechanochemical engines, transforming pH changes into mechanical work against hydrostatic pressure. As the resilin bands interlaminate with bands of cuticle, changes in resilin volume are constrained to a single direction along the air-sac's longitudinal axis. This makes the air-sac functionally equivalent to a cross-striated pH muscle and demonstrates a unique biological role for resilin as an active structural element.

RESULTS AND DISCUSSION

Air-sac volume is altered by changing the pH of resilin

Phantom midges (genus *Chaoborus*) occur globally and are members of the Chaoboridae,[7] an ancient sister group to the mosquitoes that evolved in the Jurassic.[8] They are the only animals other than fish that have evolved the ability to regulate their buoyancy using compressible gas-filled bladders. Each larva possesses four air-sacs, an anterior pair in the thorax and a posterior pair in the 7th abdominal segment. The air-sacs are derived from the longitudinal tracheal trunks of the larva's respiratory system.[5,6] However, they share no pneumatic connection to the rest of the insect's reduced tracheal system[5,6] and serve no respiratory function.[1] The wall of the air-sac, like that of the tracheal system, is made from cuticle. Unusually, the air-sac wall also incorporates bands of protein between the bands of chitinous cuticle (Figure 1D). We identified this protein as resilin: a disorganized, crosslinked protein found in arthropods that functions as a near-perfect biological rubber[9] for storing elastic energy[10] in fatigue-resistant articulations and hinges.[11]

Resilin fluoresces under UV light due to the presence of the di- and tri-tyrosine bonds that crosslink its protein chains.[12] Air-sacs exposed to violet (380 nm) or UV (360–370 nm) light emitted a bright blue fluorescence typical of this protein (Figures 2B, 2C, and 2E). Crucially for the air-sacs' function, resilin also displays reversible pH-dependent swelling.[13] By exposing excised air-sacs to a series of pH buffers, we found that their sagittal cross-sectional area changed with pH in the same manner as other insect resilins (Figure 1A; Video S1).[13] Air-sacs were smallest at pH 4, shrinking by 19.7% ± 2.0 relative to their area at pH 7 and coinciding with the isoelectric point of resilin (Figure 1A)[13] but increasing in area both above and below this pH. We found area increased by a maximum 44.4% ± 9.9 at pH 10 relative to area at pH 7, but deformation of the air-sac wall at pH 11 interfered with further measurement. Varying ionic strength (IS) also caused volume changes. However, increasing IS by 10^6 mM only resulted in an 8.1% ± 2.2 decrease in area, with the greatest change occurring below 0.1 mM, well below biologically relevant IS (Figure 1A). The presence of resilin in the air-sac wall provides the mechanism for altering the volume of the air-sac, which secondarily causes gas to passively move in or out; when the air-sac's wall expands outward, the gas pressure within the air-sac falls, allowing dissolved gases in the surrounding hemolymph to passively diffuse inward down their partial pressure gradients. Conversely, contraction of the wall raises the pressure and causes gas to diffuse out. Thus, for *Chaoborus* larvae to regulate their buoyancy, they need only possess the ability to manipulate the pH of the air-sac wall.

Please cite this article in press as: McKenzie et al., A pH-powered mechanochemical engine regulates the buoyancy of *Chaoborus* midge larvae, Current Biology (2022), https://doi.org/10.1016/j.cub.2022.01.018

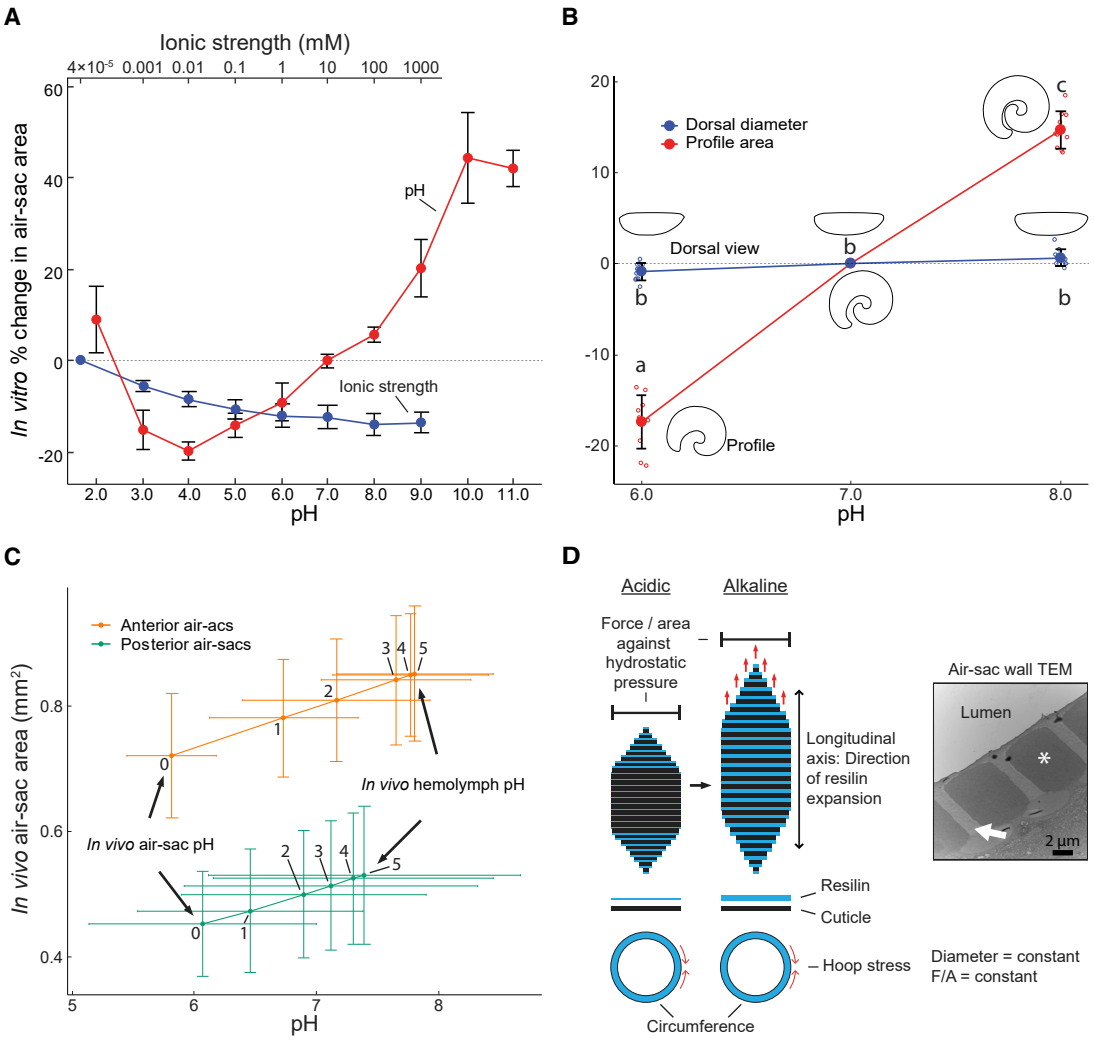

Figure 1. Changes in air-sac dimensions in response to pH changes

(A) pH and ionic strength (IS). Red: air-sacs placed in standard pH buffers and allowed to equilibrate for 5 min before measurement. Means shown are pooled averages of all four air-sacs from each individual larva. Air-sac areas are standardized to the mean value at pH 7. The smallest air-sac size and resilin's isoelectric point occur at pH 4, with air-sacs expanding at higher or lower pH values. See also Video S1. Blue: Air-sacs placed in square walled capillary tubes were flushed with lysis buffer to remove their endothelia and then subjected to increasing IS using NaCl solutions. Differences are shown as % changes from area at the IS of reverse osmosis (RO) water.

(B) Change in air-sac size shown by growth in profile area while diameter remains constant. Different lower-case letters indicate significant differences in mean value (where pMCMC <0.05). Markov chain Monte Carlo (MCMC) generalized linear mixed effects models were used to evaluate results. For the apparatus which contained air-sacs during measurement, see also Figure S2.

(C) The relationship between air-sac profile area and pH. Air-sac area was recorded in intact larvae before injection with DMSO and artificial hemolymph (AH, see also Methods S1) and every hour until 5 hours afterward. Air-sacs were then excised, and area was recorded after equilibration in three standard pH buffers (pH 6.0, 7.0, and 8.0). The linear relationship between pH and area was then calculated, revealing *in vivo* air-sac pH.

(D) A schematic showing the organization of cuticle and resilin within an air-sac and how this results in work being performed in one dimension only. Diameter, and therefore hoop stress, remains constant as length changes. A transmission electron microscopy (TEM) image of a section through the air-sac wall shows the bands of cuticle (arrow) and resilin (asterisk), and a scale bar at the bottom right indicates size of the structure.

Data are indicated as means, and error bars show ± SD.

See also Figure S2, Methods S1, and Video S1.

The air-sac endothelium regulates pH via VHA and cAMP

Each air-sac is completely enveloped by an endothelium. Immunofluorescent labeling revealed that this tissue stains strongly for vacuolar type H^+ V-ATPase (VHA), a proton-translocating enzyme that is ubiquitous among eukaryotes (Figures 2B and 2E; Video S2).[14] In insects, proton transport by VHA energizes membranes for a variety of ion transport purposes, including generating pH changes in extracellular spaces like the gut lumen.[15–17] To test whether the endothelium transports protons apically to lower the pH of the air-sac wall, we dissected intact air-sacs into artificial hemolymph (AH; pH 7.4) then exposed them to 1 µM Carbonyl

Please cite this article in press as: McKenzie et al., A pH-powered mechanochemical engine regulates the buoyancy of *Chaoborus* midge larvae, Current Biology (2022), https://doi.org/10.1016/j.cub.2022.01.018

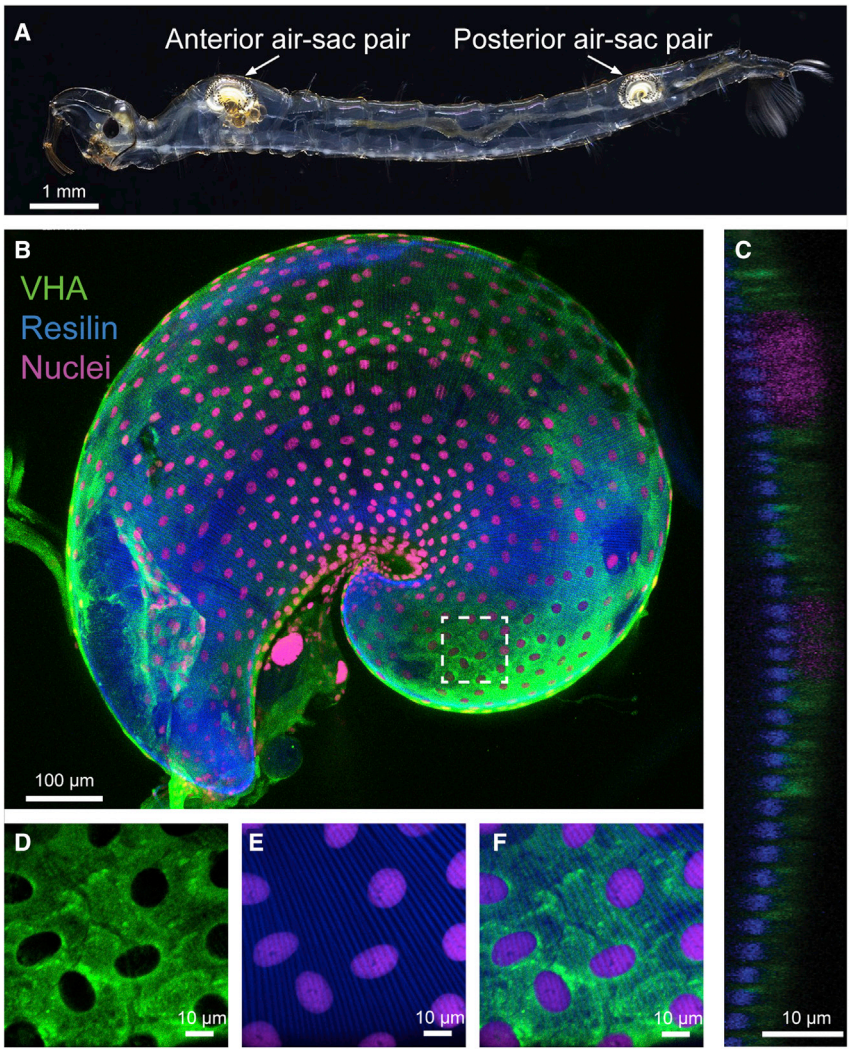

Figure 2. Whole animal, immunofluorescence, and TEM images of Chaoborus and associated air-sacs

(A) Fourth instar *Chaoborus americanus* larva showing left-hand side anterior and posterior air-sacs.

(B) Confocal immunofluorescence of an intact air-sac showing VHA (green), resilin bands (blue), and nuclei (magenta).

(C) The same air-sac as in (B) with the image plane perpendicular to the air-sac wall and direction of resilin banding to show the air-sac wall and endothelium in apposition.

(D) Closeup of (B) showing VHA staining.

(E) Closeup of (B) showing nuclei and bands of resilin.

(F) Combined images (B) and (C). A 3D animation of confocal images (Video S2) is provided as supplementary material.

Scale bars at the bottom of each image indicate size. For antibody validation, see also Figure S1.

cyanide-*p*-trifluoromethoxyphenylhydrazone (FCCP), a protonophore that dissipates transmembrane proton gradients. This caused the air-sacs to expand by 12.7% ± 4.4 relative to controls (Figure 3A), confirming air-sac acidification *in vivo*. The solvent DMSO, which also increases lipid membrane permeability to protons,[18] induced a smaller but still significant 2.5% ± 2.4 expansion of excised air-sacs relative to controls (Figure 3A). We then microinjected larvae with DMSO to increase the permeability of the air-sac endothelia *in situ*. A final hemolymph concentration of ~3% DMSO caused an expansion of anterior air-sacs by 18.2% ± 4.7 and posterior air-sacs by 17.2% ± 4.9 as the pH of the air-sac wall approached that of the more alkaline hemolymph over 5 h (Figure 1C). Following this treatment, the air-sacs were excised and exposed to a series of pH buffers (pH 6.0, pH 7.0, and pH 8.0), revealing the specific pH/area relationship for each air-sac. This information allowed us to calculate that, before DMSO injection, the air-sac's *in vivo* pH was 5.7 ± 0.4 and 6.1 ± 0.9 (anterior and posterior, respectively), but following endothelial permeabilization, pH increased significantly to 7.72 ± 0.6 and 7.4 ± 1.3 (Figure 1C). Finally, microinjecting bafilomycin, a potent VHA inhibitor, into the hemolymph caused significant air-sac expansion of 9.9% ± 5.6 relative to controls injected with AH (Figure 3B). These experiments all indicate that VHA maintains the air-sac pH substantially below that of the alkaline hemolymph.

To investigate the cellular signaling pathways which modulate the air-sac's pH, and therefore its volume, excised air-sacs were placed individually into square-walled borosilicate glass capillary tubes filled with AH. In AH, the air-sacs gradually contracted due to baseline VHA-mediated acidification, as shown prior to drug exposure (Figure 3C). Flushing the capillary with 1 µM bafilomycin (Figure 3C) caused significant expansion and confirmed the role of VHA in air-sac acidification. As the cyclic nucleotides cyclic adenosine monophosphate (cAMP) and cyclic guanosine monophosphate (cGMP) are known to regulate VHA activity in other insect tissues,[19–23] air-sacs were exposed to 1 mM 8-Bromo-cGMP and 8-Bromo-cAMP. While 8-Bromo-cGMP had no significant effect on sac area, 8-Bromo-cAMP caused significant air-sac expansion of 12.5% ± 9.0 relative to controls (Figure 3D). Increasing endogenous cAMP using a combination of 0.1 mM of the potent adenylyl cyclase activator forskolin and 0.5 mM of the phosphodiesterase inhibitor 1-Methyl-3-Isobutylxanthine (IBMX) also caused expansion of 6.4% ± 2.8 (Figure 3D). Within the cell, cAMP may activate a variety of downstream effectors, including protein kinase A (PKA) and exchange proteins directly activated by cAMP (Epac). We conducted experiments using cAMP analogs which preferentially activate either PKA or Epac to examine downstream signaling which leads to air-sac expansion. Air-sacs exposed to 0.5 mM of the Epac-specific cAMP analog 8-pCPT-2'-O-Me-Cyclic AMP (8-pCPT) for 2 h significantly increased in area by 6.7% ± 6.4 relative to controls, which showed no significant change (Figure 3D). Air-sacs exposed to 0.5 mM of the PKA-specific cAMP analog

Please cite this article in press as: McKenzie et al., A pH-powered mechanochemical engine regulates the buoyancy of *Chaoborus* midge larvae, Current Biology (2022), https://doi.org/10.1016/j.cub.2022.01.018

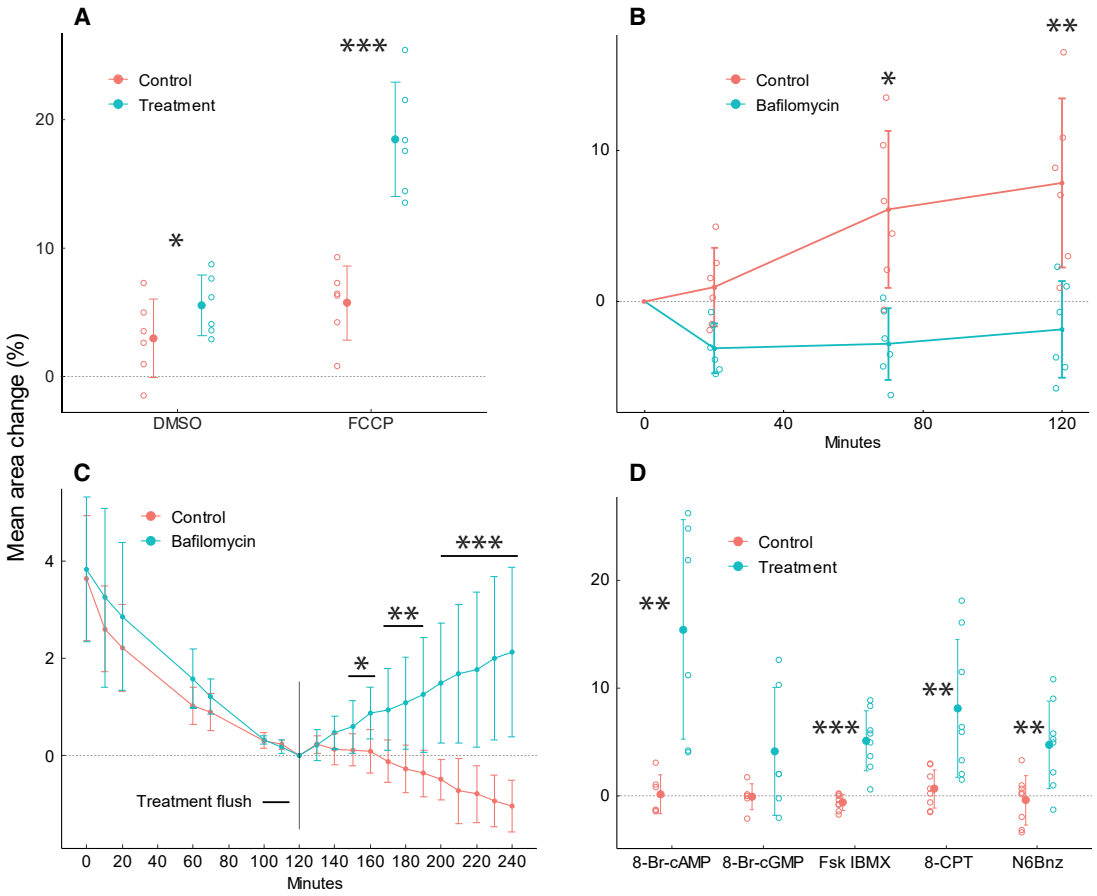

Figure 3. The effects of solvents, inhibitors, and stimulants on endothelial ability to maintain a pH gradient between the air-sac wall and hemolymph

(A) Air-sacs placed in droplets of artificial hemolymph (AH, see also Methods S1) either containing no drug or containing the protonophore FCCP or solvent DMSO. Air-sacs were exposed to FCCP or DMSO for 60 min.

(B) Intact larvae were injected with bafilomycin to a hemolymph concentration of approximately 50 μM or with control AH (see also Methods S1). Larvae were placed in high viscosity methyl cellulose for manipulation and rotated so that the air-sacs on the right side of the animal were facing upward for imaging. Images were taken prior to injection, and 20, 70, and 120 min after injection.

(C) Posterior air-sacs were excised and placed in square-walled capillary tubes (see also Figure S2 for an approximation of the apparatus used) flushed with AH (see also Methods S1) and allowed to equilibrate for 120 min. AH containing 1 μM bafilomycin was then flushed past the treatment air-sacs and compared to control air-sacs from the same animals exposed to control AH.

(D) The same experimental design as in (C) was used to evaluate air-sac expansion caused by 8-Bromo-cAMP, 8-Bromo-cGMP, forskolin + IBMX, 8-CPT, and N6Bnz (see also Methods S1). For evidence of the independent effects of 8-CPT and N6Bnz, see also Figure S3. Final time points at 240 min are shown.

Asterisks represent significant differences between treatment and control groups (where pMCMC < 0.05). MCMC generalized linear mixed effects models were used to evaluate results. * pMCMC < 0.05, ** pMCMC < 0.01, *** pMCMC < 0.001.

Data are indicated as means, and error bars show ± SD.

See also Figures S2 and S3 and Methods S1.

N^6-benzoyl-Cyclic AMP (N6Bnz) also expanded significantly (5.5% ± 4.0 relative to controls; Figure 3D). Although cAMP is known to activate VHA in other secretory epithelia,[23–26] this pathway would lead to contraction rather than expansion of *Chaoborus* air-sacs. Thus, our results indicate that both cAMP effectors play a role in increasing the pH of the air-sac wall through pathways that remain to be identified.

pH determines resilin swelling state via ionization

Chaoborus air-sacs must perform under pressure, as lake-dwelling larvae undertake diel vertical migrations[27,28] subjecting their air-sacs to significant pressures at depth. Furthermore, the larvae of one species, *C. edulis* of Lake Malawi in east Africa, routinely descend 250 m below the surface,[29] experiencing a crushing 24 atmospheres of hydrostatic pressure. For the air-sacs to resist collapsing at these depths, this pressure must be opposed by either the rigidity of the air-sac wall or an increase in internal air-sac pressure. However, as gases diffuse freely across the air-sac wall,[1,2] the pressure within the air-sac cannot be increased to counterbalance hydrostatic pressure at any depth. This is because both the total pressure and composition of the gases within the air-sac are in equilibrium with the gases dissolved in the surrounding water (~1 atm in air-equilibrated water). Increasing the pressure above 1 atm will simply cause

the gases within the air-sac to diffuse out, down their respective partial pressure gradients. As a result, the air-sac wall must withstand the hydrostatic pressure unassisted.

Consequently, to regulate buoyancy at depth, the air-sac wall must be capable of generating a force that exceeds the hydrostatic pressure to expand outward. There are currently no data regarding the pressure resilin exerts by expansion as a result of alkalinization, but in the case of *C. edulis*, it must produce an order of magnitude more force than insect striated muscle, which produces a mean specific tension equivalent to 1.8 atmospheres of pressure.[30] In resilin, the energy necessary to perform the work of expansion comes from changes in the ionization state of its constituent amino acids. In an analogous system based on crosslinked polyacrylic acid, the complete neutralization of its acidic groups would generate an osmotic pressure on the order of one hundred atmospheres.[31] Because resilin behaves as a cross-linked amphoteric polyelectrolyte, exposing it to a high pH ionizes its acidic residues.[11] With more negatively charged amino acids in alkaline media, the network's hydrophilicity (ability to bind water) increases,[32,33] a Donnan-osmotic effect develops due to cations surrounding the newly formed negative charges in the network,[34] and swelling occurs. Decreasing the pH reverses this process.

Air-sacs expand in one dimension only

While a simple block of resilin swells and contracts isometrically in all dimensions, we found that because the air-sac wall is comprised of alternating layers of resilin and stiff cuticle, changes in dimension occur in its long-axis only. We exposed excised air-sacs to three different pHs (6.0, 7.0, and 8.0) after removing their endothelia using lysis buffer. At each pH, we recorded the air-sac's sagittal cross-sectional area and its diameter as measured from the dorsal view at the widest point. We found that air-sac diameter did not change significantly (< 1%) with changes in pH, but sagittal cross-sectional areas relative to those at pH 7 decreased by 17.3% ± 3.0 in pH 6 and increased by 14.7% ± 2.0 in pH 8 (Figure 1B). So, while changes in air-sac volume are free to occur perpendicular to the bands of cuticle, circumferential expansion is prevented. Remarkably, an artificial mechanochemical system termed a cross-striated pH muscle based on exactly these principles was described in 1960,[34] composed of alternating layers of ionizable polyvinyl alcohol and strongly crosslinked polyacrylic acid. This banded arrangement is analogous to that of the sarcomeres in striated muscle, except that, unlike muscle, the air-sac wall exerts force in both contraction and expansion.

The arrangement of resilin in layers between rigid cuticle also confers three key advantages for air-sac function. First, the air-sac maintains a constant diameter in transverse cross-section (perpendicular to the air-sac's long axis), even as its length, and therefore volume, changes (Figure 1D). This is significant because the circumferential wall stress (hoop stress σ_h) required to withstand a given hydrostatic pressure is proportional to the diameter of the wall, as $\sigma_h = PD/2T$, where P is the external pressure, D is the diameter, and T is the wall thickness. If the air-sac wall were simply homogeneous resilin with no cuticle or banding, its diameter would increase along with its length. At constant P, this would lead hoop stress to increase, potentially to the point of air-sac failure. The relation of σ_h to D likely explains why the air-sacs of *Chaoborus* species from shallow ponds are bulbous and kidney-shaped while deep-water species possess longer, narrower air-sacs that curl in on themselves.[35] Second, as the resilin exerts force only in the direction of the air-sac's long axis, the force required to expand the air-sac remains constant for a given P as volume increases (Figure 1D), unlike circumferential expansion where D, and thus σ_h, would increase. Third, because the longitudinal stress (σ_L) of a cylinder is only half of σ_h ($\sigma_L = PD/4T$), the force the resilin bands must exert to expand the air-sac's longitudinal axis against hydrostatic pressure is only half that required for circumferential expansion.

While striated mechanochemical engines based on synthetic polymers have been studied for decades,[36] the hydrostatic air-sacs of *Chaoborus* are the first example found in nature. It is also the only known instance of resilin functioning as a pH-powered actuator *in vivo*, a fact that makes this protein a potentially valuable pH-driven, muscle-mimetic biomaterial.[37] Recombinant *Drosophila melanogaster* resilin has already demonstrated functionality in pH responsive materials,[33] despite functioning solely as an elastomer in this insect.[38] We suggest that *Chaoborus* resilin, which evolved to transform pH changes into mechanical work, could be the basis for a biomaterial that is optimized for use in pH-sensing or pH-driven applications. Furthermore, determining how the structure of *Chaoborus* resilin relates to its unique function would allow resilin-mimetic polypeptides to be engineered incorporating these desirable properties. Finally, understanding how this unique mechanochemical system functions may yield profound insights into how novel secretory epithelia, and their regulatory mechanisms, evolve.

STAR★METHODS

Detailed methods are provided in the online version of this paper and include the following:

- KEY RESOURCES TABLE
- RESOURCE AVAILABILITY
  - Lead contact
  - Materials availability
  - Data and code availability
- EXPERIMENTAL MODEL AND SUBJECT DETAILS
- METHOD DETAILS
  - Artificial hemolymph (AH) for *in vitro* live tissue, pH 7.4
  - Dissection and preparation of air-sacs
  - Immunostaining and imaging
  - Effect of a pH series on air-sac profile area
  - Effect of changing ionic strength on air-sac profile area
  - Comparison of changes in air-sac length versus diameter
  - *In vitro* drug exposure in square capillary tubes
  - Treatment of excised air-sacs in droplets containing FCCP and DMSO
  - Estimation of resilin and hemolymph pH
  - *In vivo* Injection of bafilomycin
- QUANTIFICATION AND STATISTICAL ANALYSIS

SUPPLEMENTAL INFORMATION

Supplemental information can be found online at https://doi.org/10.1016/j.cub.2022.01.018.

ACKNOWLEDGMENTS

Thanks to Natalie Schimpf and Christian Damsgaard for translating German and Danish papers. This study was funded by the Natural Sciences and Engineering Research Council of Canada, discovery grants RGPIN-2014-05794 and RGPIN-2020-07089 (P.G.D.M) and discovery accelerator supplement RGPAS-462242-2014 and RGPAS-2020-00039 (P.G.D.M); British Columbia Graduate Scholarship (E.K.G.M); National Science Foundation Graduate Research Fellowship Program (G.T.K); and the NSF Postdoctoral Research Fellowship in Biology Award no. 1907334 (G.T.K).

AUTHOR CONTRIBUTIONS

Conceptualization: E.K.G.M and P.G.D.M; investigation: E.K.G.M, G.T.K, M.T., and P.G.D.M; visualization: E.K.G.M, G.T.K, M.T., and P.G.D.M; funding acquisition: P.G.D.M; project administration: E.K.G.M and P.G.D.M; supervision: P.G.D.M; writing – original draft: E.K.G.M and P.G.D.M; writing – review & editing: E.K.G.M, P.G.D.M, G.T.K, and M.T.

DECLARATION OF INTERESTS

The authors declare no competing interests.

Received: October 14, 2021
Revised: December 19, 2021
Accepted: January 7, 2022
Published: January 25, 2022

REFERENCES

1. Krogh, A. (1911). On the hydrostatic mechanism of the *Corethra* larva with an account of methods of microscopical gas analysis. Skand. Arch. Physiol. *25*, 183–203.
2. Teraguchi, S. (1975). Correction of negative buoyancy in phantom larva, *Chaoborus americanus*. J. Insect Physiol. *21*, 1659–1670.
3. Teraguchi, S. (1975). Detection of negative buoyancy in phantom larva, *Chaoborus americanus*. J. Insect Physiol. *21*, 1265–1269.
4. Christensen, P. (1928). Bidrag til Kendskabet om Corethralarvens hydrostatiske Mekanisme. Vidensk. Meddr dansk naturh. Foren. *86*, 21–48.
5. Damant, G.C.C. (1924). The adjustment of the buoyancy of the larva of *Corethra plumicornis*. J. Physiol. *59*, 345–356.
6. Von Frankenberg, G. (1915). Die Schwimmblasen von Corethra (Fischer).
7. Saether, O.A. (2000). Phylogeny of Culicomorpha (Diptera). Syst. Entomol. *25*, 223–234.
8. Borkent, A. (1993). A world catalog of fossil and extant Corethrellidae and Chaoboridae (Diptera), with a listing of references to keys, bionomic information and descriptions of each known life stage. Entomol. Scand. *24*, 1–24.
9. Weis-Fogh, T. (1961). Thermodynamic properties of resilin, a rubber-like protein. J. Mol. Biol. *3*, 520–531.
10. Bennet-Clark, H.C., and Lucey, E.C.A. (1967). The jump of the flea: a study of the energetics and a model of the mechanism. J. Exp. Biol. *47*, 59–67.
11. Andersen, S.O., and Weis-Fogh, T. (1964). Resilin. A Rubberlike Protein in Arthropod Cuticle. In Advances in Insect Physiology, *Volume 2*, J.W.L. Beament, J.E. Treherne, and V.B. Wigglesworth, eds. (Academic Press), pp. 1–65.
12. Andersen, S.O. (1964). The cross-links in resilin identified as dityrosine and trityrosine. Biochim. Biophys. Acta *93*, 213–215.
13. Weis-Fogh, T. (1960). A rubber-like protein in insect cuticle. J. Exp. Biol. *37*, 889–907.
14. Nelson, N., and Taiz, L. (1989). The evolution of H^+-ATPases. Trends Biochem. Sci. *14*, 113–116.
15. Boudko, D.Y., Moroz, L.L., Harvey, W.R., and Linser, P.J. (2001). Alkalinization by chloride/bicarbonate pathway in larval mosquito midgut. Proc. Natl. Acad. Sci. USA *98*, 15354–15359.
16. Harvey, W.R. (2009). Voltage coupling of primary H^+ V-ATPases to secondary Na^+- or K^+-dependent transporters. J. Exp. Biol. *212*, 1620–1629.
17. Wieczorek, H. (1992). The insect V-ATPase, a plasma membrane proton pump energizing secondary active transport: molecular analysis of electrogenic potassium transport in the tobacco hornworm midgut. J. Exp. Biol. *172*, 335–343.
18. Ma, L., Dong, J.-X., Fu, W.-R., Li, X.-Y., Chen, J., and Liu, Y. (2018). Mitochondrial morphology and function impaired by dimethyl sulfoxide and dimethyl Formamide. J. Bioenerg. Biomembr. *50*, 297–305.
19. Berridge, M.J., and Patel, N.G. (1968). Insect salivary glands: stimulation of fluid secretion by 5-hydroxytryptamine and adenosine-3',5'-monophosphate. Science *162*, 462–463.
20. Dames, P., Zimmermann, B., Schmidt, R., Rein, J., Voss, M., Schewe, B., et al. (2006). cAMP regulates plasma membrane vacuolar-type H^+-ATPase assembly and activity in blowfly salivary glands. Proc. Natl. Acad. Sci. USA *103*, 3926–3931.
21. Dow, J.A., Maddrell, S.H., Davies, S.A., Skaer, N.J., and Kaiser, K. (1994). A novel role for the nitric oxide-cGMP signaling pathway: the control of epithelial function in *Drosophila*. Am. J. Physiol. *266*, R1716–R1719.
22. Rein, J., Voss, M., Blenau, W., Walz, B., and Baumann, O. (2008). Hormone-induced assembly and activation of V-ATPase in blowfly salivary glands is mediated by protein kinase A. Am. J. Physiol. Cell Physiol. *294*, C56–C65.
23. Tiburcy, F., Beyenbach, K.W., and Wieczorek, H. (2013). Protein kinase A-dependent and -independent activation of the V-ATPase in Malpighian tubules of *Aedes aegypti*. J. Exp. Biol. *216*, 881–891.
24. Gong, F., Alzamora, R., Smolak, C., Li, H., Naveed, S., Neumann, D., Hallows, K.R., and Pastor-Soler, N.M. (2010). Vacuolar H^+-ATPase apical accumulation in kidney intercalated cells is regulated by PKA and AMP-activated protein kinase. Am. J. Physiol. Renal Physiol. *298*, F1162–F1169.
25. Schewe, B., Schmälzlin, E., and Walz, B. (2008). Intracellular pH homeostasis and serotonin-induced pH changes in *Calliphora* salivary glands: the contribution of V-ATPase and carbonic anhydrase. J. Exp. Biol. *211*, 805–815.
26. Tresguerres, M., Levin, L.R., and Buck, J. (2011). Intracellular cAMP signaling by soluble adenylyl cyclase. Kidney Int. *79*, 1277–1288.
27. Juday, C. (1921). Observations on the larvae of *Corethra punctipennis* Say. Biol. Bull. *40*, 271–286.
28. Teraguchi, M., and Northcote, T.G. (1966). Vertical distribution and migration of *Chaoborus flavicans* larvae in Corbett Lake, British Columbia. Limnol. Oceanogr. *11*, 164–176.
29. Irvine, K. (1997). Food selectivity and diel vertical distribution of *Chaoborus edulis* (Diptera, Chaoboridae) in Lake Malawi. Freshw. Biol. *37*, 605–620.
30. Rospars, J.-P., and Meyer-Vernet, N. (2016). Force per cross-sectional area from molecules to muscles: a general property of biological motors. R. Soc. Open Sci. *3*, 160313.
31. Wassermann, A. (1960). Size and Shape Changes of Contractile Polymers: Conversion of Chemical Into Mechanical Energy. In Proceedings of Seminars [on Polymer Science] Held at University College, London [July 1957 and April 1958] (Pergamon Press), pp. 41–77.
32. Balu, R., Dutta, N.K., Choudhury, N.R., Elvin, C.M., Lyons, R.E., Knott, R., and Hill, A.J. (2014). An16-resilin: an advanced multi-stimuli-responsive resilin-mimetic protein polymer. Acta Biomater. *10*, 4768–4777.
33. Truong, M.Y., Dutta, N.K., Choudhury, N.R., Kim, M., Elvin, C.M., Hill, A.J., Thierry, B., and Vasilev, K. (2010). A pH-responsive interface derived from resilin-mimetic protein Rec1-resilin. Biomaterials *31*, 4434–4446.
34. Kuhn, W., Ramel, A., Walters, D.H., Ebner, G., and Kuhn, H.J. (1960). The production of mechanical energy from different forms of chemical energy with homogeneous and cross-striated high polymer systems (Berlin, Heidelberg: Springer Berlin Heidelberg).

35. Bardenfleth, K.S., and Ege, R. (1916). On the anatomy and physiology of the air-sacs of *Corethra plumicornis*. Vidensk Medd fra Dansk naturh Foren *67*, 25–42.
36. Walters, D.H., Kuhn, W., and Kuhn, H.J. (1961). Action potential with an artificial pH-muscle. Nature *189*, 381–383.
37. Lv, S., Dudek, D.M., Cao, Y., Balamurali, M.M., Gosline, J., and Li, H. (2010). Designed biomaterials to mimic the mechanical properties of muscles. Nature *465*, 69–73.
38. Lerch, S., Zuber, R., Gehring, N., Wang, Y., Eckel, B., Klass, K-D., et al. (2020). Resilin matrix distribution, variability and function in *Drosophila*. BMC Biol. *18*, 195.
39. Armstrong, E.J., Roa, J.N., Stillman, J.H., and Tresguerres, M. (2018). Symbiont photosynthesis in giant clams is promoted by V-type H^+-ATPase from host cells. J. Exp. Biol. *221*, jeb177220.
40. Fedorenko, A.Y., and Swift, M.C. (1972). Comparative biology of *Chaoborus americanus* and *Chaoborus trivittatus* in Eunice Lake, British Columbia. Limnol. Oceanogr. *17*, 721–730.
41. Saether, O.A. (1972). Chaoboridae. In Das Zooplankton der Binnengewässer. I Teil. Die Binnengewässer, *26*, pp. 257–280.
42. Scholz, F., and Zerbst-Boroffka, I. (1998). Environmental hypoxia affects osmotic and ionic regulation in freshwater midge-larvae. J. Insect Physiol. *44*, 427–436.
43. Barott, K.L., Venn, A.A., Perez, S.O., Tambutté, S., and Tresguerres, M. (2015). Coral host cells acidify symbiotic algal microenvironment to promote photosynthesis. Proc. Natl. Acad. Sci. USA *112*, 607–612.
44. Damsgaard, C., Lauridsen, H., Harter, T.S., Kwan, G.T., Thomsen, J.S., Funder, A.M.D., Supuran, C.T., Tresguerres, M., Matthews, P.G.D., and Brauner, C.J. (2020). A novel acidification mechanism for greatly enhanced oxygen supply to the fish retina. eLife *9*, e58995.
45. Thomsen, J., Himmerkus, N., Holland, N., Sartoris, F.J., Bleich, M., and Tresguerres, M. (2016). Ammonia excretion in mytilid mussels is facilitated by ciliary beating. J. Exp. Biol. *219*, 2300–2310.
46. Daniolos, A., Lerner, A.B., and Lerner, M.R. (1990). Action of light on frog pigment cells in culture. Pigment Cell Res. *3*, 38–43.
47. Kashina, A.S., Semenova, I.V., Ivanov, P.A., Potekhina, E.S., Zaliapin, I., and Rodionov, V.I. (2004). Protein kinase A, which regulates intracellular transport, forms complexes with molecular motors on organelles. Curr. Biol. *14*, 1877–1881.

Please cite this article in press as: McKenzie et al., A pH-powered mechanochemical engine regulates the buoyancy of *Chaoborus* midge larvae, Current Biology (2022), https://doi.org/10.1016/j.cub.2022.01.018

STAR★METHODS

KEY RESOURCES TABLE

REAGENT or RESOURCE	SOURCE	IDENTIFIER
Antibodies		
Anti-VHA subunit B	[39]	N/A
Chemicals, peptides, and recombinant proteins		
Bafilomycin A1	Cayman Chemical	11038
Forskolin	Sigma	F6886
IBMX	Cayman Chem	13347
8-Bromo-cGMP	Cayman Chem	15992
8-Bromo-cAMP	Cayman Chem	41131
8-pCPT-2'-O-Me-Cyclic AMP	Cayman Chem	17143
N6-benzoyl-Cyclic AMP	Cayman Chem	18819
FCCP	Sigma-Aldrich	Cat# C2920
DMSO	Sigma-Aldrich	D5879
Methylcellulose 1500 cPs	Sigma-Aldrich	Cat# M0387
Triton X-100 lysis buffer	Alfa Aesar	J62289
NaCl	VWR	0251-1
KCl	MilliporeSigma	PX1405-1
$CaCl_2$	VWR	18706-300
$MgCl_2$	Fisher Chemical	M33-500
$NaHCO_3$	G-biosciences	RC-091
HEPES	Fisher Chemical	7365-45-9
L-Malic Acid	Sigma-Aldrich	M7397
NaOH	Sigma-Aldrich	221465
Glucose	Sigma-Aldrich	G7021
Deposited data		
Raw Data	This Paper	Figshare: https://doi.org/10.6084/m9.figshare.16679986.v1
Experimental models: Organisms/strains		
Wild caught *Chaoborus americanus* larvae	UBC research ponds	N/A
Wild caught *Chaoborus trivittatus* larvae	Malcolm Knapp Research Forest	N/A
Software and algorithms		
ImageJ	National Institutes of Health	https://imagej.nih.gov/ij/
R 4.0.2	CRAN	https://www.r-project.org/
Other		
Inverted Microscope	Olympus	IX73
Dissecting Microscope	Olympus	SZX2-ILLT
Inverted Confocal Microscope	Zeiss	AxioObserver Z1

RESOURCE AVAILABILITY

Lead contact

Further information and requests for resources and reagents should be directed to and will be fulfilled by the lead contact, Evan K. G. McKenzie (emckenzie@zoology.ubc.ca)

Materials availability

This study did not generate new unique reagents

Please cite this article in press as: McKenzie et al., A pH-powered mechanochemical engine regulates the buoyancy of *Chaoborus* midge larvae, Current Biology (2022), https://doi.org/10.1016/j.cub.2022.01.018

Data and code availability

Experimentally generated data have been deposited at Figshare and are publicly available as of the date of publication. The DOI (Figshare: https://doi.org/10.6084/m9.figshare.16679986.v1) is also listed in the key resources table.

This paper does not report original code.

Any additional information required to reanalyze the data reported in this paper is available from the lead contact upon request.

EXPERIMENTAL MODEL AND SUBJECT DETAILS

Third and fourth instar *Chaoborus americanus* larvae were collected from 6 m-deep experimental ponds located at UBC Point Grey Campus (49°14'51.9"N 123°13'59.2"W) using a 12" diameter × 38" long, 153 μm mesh plankton tow net. These larvae were used for the experiment exposing air-sacs to a pH series to determine the air-sac swelling curve and isoelectric point, as well as determining the effect of ionic strength (IS) on air-sac swelling. All other experiments were conducted using fourth instar *Chaoborus trivittatus.* These were collected from Shirly Lake in the UBC Malcolm Knapp Research Forest (49°20'43.5"N 122°33'40.8"W) located in Maple Ridge, British Columbia, Canada, using a 12" diameter × 42" long, 243 μm mesh plankton tow net. The larvae were transported to the laboratory and maintained in dechlorinated Vancouver tap water at 10°C until use. After approximately 24 h, to avoid water fouling, once the debris and other swimming invertebrates caught along with the *Chaoborus* had settled out, the larvae were transferred to fresh water free of detritus. Larvae were identified as *C. trivittatus* or *C. americanus* using descriptions from Fedorenko and Swift[40] and Saether.[41] Sex was not determined as sex differences do not become apparent until adulthood.

METHOD DETAILS

Artificial hemolymph (AH) for *in vitro* live tissue, pH 7.4

Based on the ion concentrations measured in *Chaoborus crystallinus* hemolymph by Scholz and Zerbst-Boroffka,[42] which include a high concentration of malate, a solution constituting artificial hemolymph (AH) was made (Methods S1), with solutes added in the order presented.

The addition of malic acid significantly lowered the pH. NaOH solution and $NaHCO_3$ powder were then added to restore the pH and provide the rest of the required Na^+. Glucose was added last to minimize bacterial activity. To allow precise pH titration, 80% of the total $NaOH_{(aq)}$ solution was initially added, with the rest added dropwise while pH was continuously measured.

Dissection and preparation of air-sacs

Larvae were placed in a Petri dish filled with artificial hemolymph solution or pH buffer, as per the experiment, and dissected by opening the body cavity using fine #5 forceps to expose the two pairs of air-sacs. For experiments that evaluated the physical effect of pH or IS, the intact end of a body segment was grasped using these forceps, allowing the air-sacs to be pushed toward the opening by pinching just behind the air-sacs using a second pair of fine forceps. For experiments where a living, intact endothelium was required, such as drug exposure, posterior air-sacs were carefully removed from their section trunk by slitting open the adjacent body wall using 2.5 mm Vannas Spring Scissors (Fine Science Tools 15000-08, North Vancouver, Canada) and freed from the body so as to minimize damage to the endothelia. Air-sacs were dissected into droplets of artificial hemolymph (AH) under a dissecting microscope (Olympus SZX2-ILLT, Tokyo, Japan).

Immunostaining and imaging

Air-sacs were dissected into droplets of 1 × PBS (Corning Incorporated, 46-013-CM, New York, USA) diluted from 10 × with RO water. Air-sacs were fixed in 4% PFA (Electron Microscopy Sciences, 15713) with 1 × PBS for 8 h at 4°C. they were then incubated in 50% ethanol for 8 h before storage in 70% ethanol. Fixed *Chaoborus* tissue was washed in PBS + 0.1% tween (PBS-T) at room temperature (RT) for 5 min, then rinsed with sodium borohydride (1.5 mg/mL) PBS-T (six times at RT; 10 min each). Next, samples were incubated in blocking buffer (PBS-T, 0.02% normal goat serum, 0.0002% keyhole limpet hemocyanin) at RT for 1 h, followed by primary antibodies against a conserved epitope in VHA subunit B (Figure S1) (1:500; 6 μg/mL) at RT overnight.[43] On the following day, samples were washed in PBS-T (three times at RT; 10 min each), incubated with goat anti-rabbit-Alexa Fluor488 secondary antibodies (1:500, Invitrogen, New York, USA), and counterstained with red nuclear dye (1:6; NucRedTM Dead 647, Invitrogen) at RT for 1 h. Samples were washed in PBS-Tx (three times at RT; 10 min each) and imaged on an inverted confocal microscope (Zeiss AxioObserver Z1 Oberkochen, Germany) connected to a laser scanner equipped with 405, 488, 561, and 640 nm laser lines (Zeiss LSM 800). The settings during image acquisition were as follows: Alexa Fluor488 was captured with excitation at 493 nm and emission detected from 510-650 nm; native resilin fluorescence was captured with excitation at 353 nm and emission detected from 410 to 510 nm; NucRed™ Dead 647 was captured with excitation at 653 nm and emission detected from 656-700 nm. 3D z stack reconstructions were generated using Zeiss ZEN 2.6 blue edition software, and Video S2 was generated using Imaris software (BitPlane, Belfast, UK). Antibody validation procedures are described in Figure S1, and references therein.[39,43–45]

Effect of a pH series on air-sac profile area

All four air-sacs from *C. americanus* larvae were dissected into a 0.25 mL droplet of pH 7 buffer solution on a microscope slide bounded with hydrophobic barrier pen. The air-sacs were allowed to equilibrate for 5 min before imaging on an inverted microscope

Please cite this article in press as: McKenzie et al., A pH-powered mechanochemical engine regulates the buoyancy of *Chaoborus* midge larvae, Current Biology (2022), https://doi.org/10.1016/j.cub.2022.01.018

at 40 × (Olympus IX73, Tokyo, Japan), using a trinocular mounted EOS R mirrorless camera (Canon, Tokyo, Japan). The solution was then removed using a micropipette and replaced with a second pH buffer. This was done twice for the second pH to rinse the air-sacs and ensure the desired pH was reached. This process was carried out from pH 2.00 to pH 11.00 at 1.0 pH unit increments and was repeated four times using air-sacs from four different larvae for each pH treatment. Profile areas of all four air-sacs from an individual were pooled as a mean in each pH treatment, allowing the difference in area resulting from the two pH treatments to be calculated. All pH buffers were RICCA reference standard pH buffers (RICCA, Arlington, USA). Changes in profile area were calculated as percentages of their values at pH 7.

Effect of changing ionic strength on air-sac profile area

A posterior air-sac from each of eight *C. americanus* larvae was dissected into reverse osmosis (RO) water, with an approximate ionic strength of 4×10^{-5} mM. This ruptured the endothelial cells before the air-sacs were placed into square walled capillary tubes for imaging (see also Figure S2). Once mounted on the microscope slide, lysis buffer with Triton® X-100 (Alfa Aesar, Massachusetts, USA) was flushed through the capillaries to ensure complete removal of the endothelium and allow full exposure of the air-sac wall to the experimental salt solutions. The lysis buffer was then rinsed away by flushing RO water through the capillary tubes. Once the air-sacs were in only RO water, they were allowed to equilibrate for 1 h, with one more rinse at 30 min, to allow as much of the native ionic solution to diffuse out of the resilin as possible. Images were taken using a trinocular mounted EOS R DSLR camera (Canon, Tokyo, Japan) on an inverted microscope at 40 × (Olympus IX73, Tokyo, Japan) at the 1-h mark to serve as a starting point to which the other measurements were normalized. Subsequently, increasing concentrations of NaCl in RO water were flushed past the air-sacs, with each solution allowed to equilibrate for 30 min before imaging. The series of ionic strengths began at 1 μM NaCl and were increased by one order of magnitude per step until 1 M NaCl was reached.

The resulting changes are plotted alongside those of the pH series, both series representing one order of magnitude steps in concentration, either of [H^+] or [NaCl].

Comparison of changes in air-sac length versus diameter

Three 0.2 M pH buffer solutions (pH 6.0, pH 7.0 and pH 8.0) were prepared from solid mono- and dibasic sodium phosphate and RO water. These were diluted to 0.1 M with RO water and titrated to the desired pH before each experiment using a digital pH meter (Seven Excellence, Mettler Toledo, Ohio, USA). All solutions were stirred using magnetic stir bar, both before and after titration, to ensure air equilibration.

One air-sac from each of ten *C. trivittatus* larvae was used for the experiment. Only posterior air-sacs were used for the experiment, as their smaller size and lack of attached lipid droplets made them ideal for imaging in the capillary tubes. The air-sacs were dissected into 0.1 M, pH 6 phosphate buffer and then transferred into 1:1 HEPES lysis buffer with Triton® X-100 (Alfa Aesar, Massachusetts, USA) and the same pH 6 phosphate buffer. The air-sacs sat in this solution for 5 min and were given a few gentle swirls in order to render the endothelium nonfunctional, but not remove it entirely. This is because the endothelium serves as a physical barrier to fluid entry at the air-sac tips as they expand. Partial flooding of the air-sac would impede its ability to equilibrate to the desired pH upon subsequent solution changes. After the treatment with lysis buffer, the air-sacs were transferred back to the pH 6 phosphate buffer as a first rinse, then to a fresh droplet of the same buffer as a second rinse. Imaging took place inside of a square walled borosilicate glass capillary (internal dimensions, 50 × 1.0 × 1.0 mm, 0.200 mm wall; 8100-050, VitroCom, NJ, USA). The air-sac was transferred into this capillary by preloading the capillary with fresh pH 6 phosphate buffer and touching its open end to the surface of the droplet containing the lysis buffered air-sac. The air-sac would then float upward into the vertical capillary tube. To arrest the air-sac's ascent upon reaching the desired location, the tube was turned horizontal. The capillary was open at one end, while the other end was connected to a length of 0.89 mm ID tubing using UV curing epoxy (Norland Optical Adhesive 68, New Jersey, USA). The tubing led to a peristaltic pump (C.P. 78001-10, Ismatec, Wertheim, Germany) allowing buffer to be drawn through the capillary. The capillary was placed in a custom-made acrylic bracket affixed to a microscope slide with UV curing epoxy, and with the open end of the capillary sitting in a drip well to receive fresh pH buffer (Figure S2). The capillary was sealed into this drip well using EXAFLEX polyvinyl siloxane (CG America Inc, Illinois USA). This setup was then placed on the stage of an inverted microscope (Olympus IX73, Tokyo, Japan) with a 40 × magnification.

With the capillary held horizontal in the slide-mounted bracket, the air-sac would float up against the upper wall of the square capillary, allowing the objective lens of the inverted microscope positioned below to view the air-sac in profile. But to image the air-sac's dorsal surface, two 3 × 3 mm right angle prisms were employed. One prism was affixed to the microscope slide adjacent to where the air-sac sits in the capillary with its vertical face next to the dorsal surface of the air-sac using Norland Optical Adhesive 68. The other prism was affixed to a second microscope slide using the same adhesive, and this was placed on top of the capillary so that it directed light from the microscope light source horizontally past the sample and into the other prism to be directed downward into the objective lens. The upper microscope slide was sealed onto the neck of the drip well using polyvinyl siloxane.

With the experimental setup placed on the inverted microscope (Olympus IX73), pH 6 buffer was placed in the drip well and the peristaltic pump was turned on, with fluid flow at a rate of 0.1 mL min^{-1}. Fresh pH 6 buffer was placed dropwise into the drip well as the solution was drawn past the air-sac. 25 drops of buffer were flushed past the air-sac, followed by a pause of approximately 1 min to allow for diffusion, followed by another flush of 25 drops. Images were taken just before the flush procedure, as well as 25 and 30 min after the end of the second flush. Air-sac size at the 30 min time point was used in the analysis, with the previous time points being for quality control, to confirm that changes in air-sac size had plateaued. After the 30 min image was taken, the stage was

Please cite this article in press as: McKenzie et al., A pH-powered mechanochemical engine regulates the buoyancy of *Chaoborus* midge larvae, Current Biology (2022), https://doi.org/10.1016/j.cub.2022.01.018

moved so that the image if the air-sac's dorsal surface could be imaged using the prism mounted on the slide. Sagittal cross-sectional area as well as diameter from the dorsal view at the widest point were measured. This process was repeated for the pH 7 and then pH 8 air-sac measurements. Changes in air-sac dimensions were then normalized to the sac sizes in pH 7.

In vitro drug exposure in square capillary tubes

To record the effect of drugs on the endothelium, air-sacs from *C. trivittatus* larvae were excised as described in the previous section and placed in square walled borosilicate glass capillary tubes (Methods S1). In this experiment, however, the acrylic frame affixed to the microscope slide contained two solution wells, each leading to two tubes. Thus, both posterior air-sacs from two different larvae could be placed in the setup, with one air-sac from each larva receiving treatment or control solutions simultaneously.

All four tubes were first flushed with control AH (Methods S1), containing an equal concentration of DMSO as the treatment solution if used, in which the air-sacs were allowed to equilibrate for 2 h, establishing a baseline area for comparison. After this, the initial solution was removed from the wells, and they were filled with either treatment (Methods S1) or control AH. The tubes were then flushed with the respective solutions and the air-sacs were allowed equilibrate for another 2 h.

The specificity of the cAMP analogs 8-pCPT and N6Bnz for Epac and PKA, respectively, are not perfect, and there may be overlap in downstream effector stimulation, depending on drug concentration. Conveniently, in addition to the endothelium, the air-sacs are surrounded by a layer of chromatophores, in which individual chromatophores may spread out to darken the air-sac, or contract into spheres, depending on environmental stimuli. Chromatophores are known to be stimulated by cAMP via PKA linked directly to pigment granules,[46,47] and this allowed us to assess whether the PKA pathway was activated. In the N6Bnz experiment, chromatophores in all air-sacs which received the treatment were caused to dilate. Conversely, this did not occur in any of the 8-pCPT stimulated air-sacs, indicating that the 8-pCPT concentration was not great enough to stimulate PKA, and that expansion was caused by Epac (Figure S3).

Treatment of excised air-sacs in droplets containing FCCP and DMSO

FCCP (C2920, Sigma-Aldrich, Missouri, USA) was obtained as 1 mM stock solution in 100% ethanol. AH was loaded with 1 μM FCCP. One anterior and one posterior air-sac from six *C. Trivittatus* larvae were placed in 25 μL droplets of this solution, and the other anterior and posterior air-sacs from each of those larvae were placed in control AH with 0.1% ethanol. Air-air-sac profiles were imaged with most of the droplet removed using a micropipette, such that the air-sacs were resting flat on the microscope slide.

The same experimental design was also used to apply 3% DMSO (Sigma D5879, St. Louis, USA) to air-sacs from six *C. trivittatus* larvae.

Imaging was done using a dissecting microscope (Olympus SZX2-ILLT, Tokyo, Japan) and EOS R mirrorless camera (Canon, Tokyo, Japan) mounted on its trinocular.

Estimation of resilin and hemolymph pH

A slightly different formula than the AH described for *in vitro* live tissue was used for *in vivo* injection (Methods S1). Rather than it being the only solution bathing the tissue, a small volume was injected into the hemolymph cavity such that differences in superfusing ion concentrations were minor.

The dose of DMSO given to larvae was based on a standard estimated larval hemolymph volume. We approximated a larval hemolymph volume of 13.5-14 μL based on previous measurements taken using ImageJ software and assuming cylindrical body segments. Larva sizes varied, and they cannot be weighed to determine dose prior to experimentation since removing them from the water results in unacceptable damage. Therefore, *in vivo* hemolymph DMSO concentration is also an approximation of ~3%.

A solution was prepared consisting of 41% DMSO and 59% insect Ringer's solution. This was injected into six larvae while another six larvae were given control insect Ringer's with no DMSO. Microinjections were carried out using a pulled borosilicate microcapillary (3.5'' × 1.14mm O.D. × 0.53mm I.D.) and a Nanoject III (Drummond Scientific Company, Pennsylvania, USA) to inject 1 μL of experimental solution into the hemolymph cavity. The tip of the pulled glass pipette was inserted between the third and fourth body segments. To restrain the larvae and support their body against the inserting force of the pipette, they were suspended in high viscosity methylcellulose (MC) 1500 cPs (Sigma-Aldrich, Missouri, USA), 3% in RO water.

Six *C. trivittatus* Larvae were placed individually in small Petri dishes filled with MC. For imaging, larvae were rotated so that the right-hand anterior and posterior air-sacs could be viewed in profile. These were imaged immediately to establish a starting point comparison. To avoid touching and damaging the delicate larvae, forceps were used to drag the MC around their bodies, causing them to rotate. This was repeated before each image because the larvae slowly right themselves through passive buoyancy and flexing of the body. Imaging was done using a dissecting microscope (Olympus SZX2-ILLT) and EOS R mirrorless camera (Canon, Tokyo, Japan) mounted on its trinocular.

After each larva was placed in the MC and initial images were taken, the injections were carried out. Images were then taken at time points of 1, 2, 3, 4 and 5 h post injection, as air-sac pH approached that of the hemolymph.

After *in vivo* air-sac areas were recorded, the larvae were placed in containers of dechlorinated Vancouver tap water to remove the MC. The air-sacs were then excised as described above and placed in lysis buffer to remove the endothelia before being placed in phosphate buffers of pH 6.0, 7.0 and then 8.0. Air-sacs were allowed to equilibrate in each of these for at least 20 min before imaging.

Please cite this article in press as: McKenzie et al., A pH-powered mechanochemical engine regulates the buoyancy of *Chaoborus* midge larvae, Current Biology (2022), https://doi.org/10.1016/j.cub.2022.01.018

From the areas measured, the specific relationship between air-sac area and pH for each air-sac was calculated using the linear formula: Area = m(pH) + b. Rearranged, this yielded the *in vivo* pH of each air-sac based on its measured area before and after the larvae were injected with DMSO.

In vivo Injection of bafilomycin

Bafilomycin A1 (11038 Cayman Chemical, Michigan, USA) was prepared in AH (same recipe as in the estimation of resilin and hemolymph pH, Methods S1) to a concentration of 1.75 mM, with a DMSO concentration of 22%. A total of 12 *C. trivittatus* larvae were used, 6 receiving bafilomycin in their injections, and 6 receiving only a solvent control. The volume injected resulted in an approximate bafilomycin concentration of 50 μM and DMSO concentration of 0.6% in the hemolymph. Microinjections were carried out as with the *in vivo* DMSO injection experiment with larvae suspended in MC to inject 0.4 μL of AH loaded with bafilomycin, or sham AH with an equivalent amount of DMSO. Images were taken of the right-hand air-sacs before injection and 20, 70 and 120 min post injection using a dissecting microscope (Olympus SZX2-ILLT) and Canon EOS R mirrorless camera (Canon, Tokyo, Japan) mounted on its trinocular.

QUANTIFICATION AND STATISTICAL ANALYSIS

MCMC generalized linear mixed effects models were used to evaluate differences between treatment effects (MCMCglmm package in R). Where air-sacs were repeatedly measured, the random effect of larval identity was accounted for, with an uninformative prior for its associated variance (V = 1, nu = 0.002 for R and G structure). Default priors were used for treatment (fixed) effects, which were essentially flat (V = 0, mu = 10^8), and therefore also uninformative. Increasing the strength of belief or other parameters did not significantly affect the results. MCMC settings were nitt = 1300000, thin = 1000, burnin = 300000. In This paper, n always represents the number of larvae, and this value can be found in each respective section of the methods. Data is indicated as mean ± SD. pMCMC values of < 0.05 were used to assess significant differences between treatment and control groups.